Rapid estimation method for span load distribution on a rectangular wing planform using tabular data from lifting-line theory

Tosaporn Soontornpasatch*
Department of Mechanical and Aerospace Engineering, Faculty of Engineer,
King's Mongkut University of Technology North Bangkok, Wongsawang, Bangsue,
Bangkok, 10800, Thailand
***Corresponding Author E-mail:** tosaporn.s@eng.kmutnb.ac.th
Received: Nov 24, 2024; **Revised:** Mar 01, 2025; **Accepted:** Mar 03, 2025

Abstract

The aim of this article is to present the rapid estimation method for span load distribution on a rectangular wing planform by using the tabular data from lifting-line theory. The data is generated by solving a monoplane equation to determine the coefficient of Fourier sine series that represents horseshoe strength distributed along the wingspan. Then the ratio of local lift coefficient to wing lift coefficient at the selected positions are determined and are presented in the tabular form. This set of data can be used to determine the spanwise lift distribution, the magnitude of total lift force and spanwise center of pressure location. The present method can be applied for a rectangular planform which has no sweep angle at quarter chord line and has no both geometric and aerodynamic twist along wingspan. The range of wing aspect ratio is 4 to 12 and the taper ratio is 0.1 to 1.0. Although the assumption of flow around wing planform is incompressible flow or at Mach number lower than 0.3, this present method can be extended to be used for subsonic compressible flow condition by using Prandtl-Glauert rule which is also discussed in this article. An illustrative example of the calculation process is presented in this article and the comparison of the result from the present method to the other calculation methods and experimental data are also discussed in this article.

Keywords: Aerodynamics, Lifting-line theory, Wingspan load distribution

1. Introduction

Calculating lift force distribution on an airplane wing is an important process in airframe structural analysis and testing. There are many situations which the distribution of lift force along wingspan has to be determined. One is the wing stress testing process in the work of Chinvorarat et al. [1], as shown in **Figure 1**. This test was performed to determine the strength of the seaplane wing. Before the testing process was performed, the lift distribution along the wingspan had to be determined and then the lift force at each specific wing station can be found. Then, they were applied in the testing process.

Figure 1 Shows the stress testing of a semi-span wing. (Picture by auther).

There are many methods that were developed in the past to determine the magnitude of lift force distributed along the wingspan. These methods are generally based on the inviscid incompressible flow theory in aerodynamics. One of the earliest and comprehensive work is the work of Anderson [2]. In this paper, the span lift distribution of a straight wing is considered to have two components. First is the basic loading distribution which depends on the wing twist at zero-lift condition. The other one is the additional loading distribution which depends on the angle of attack of wing. When these two components are known, the lift distribution can be determined. Another comprehensive works are the works of DeYoung [3] and Stevens [4]. These two papers show the method of calculation for theoretical basic span loading and additional span loading of arbitrary sweep wing at various taper, sweep angle and aspect ratio. Both works are based on the work of Weissinger [5] which used modified lifting line method to determine spanwise loading distribution. All these works were summarized in the work of DeYoung and Harper [6] which shows the complete process for calculating span lift distribution and other important aerodynamic parameters in detail.

Although the methods in all these works were developed to be used as a manual calculation method and can be applied without using a computer. They are still difficult to use. This comes from the fact that they were created for arbitrary wing planform that has the effect of wing twist and includes the effect of sweep

angle. Therefore, the calculation process is very complex which involves a lot of tables and graphs. This causes an inconvenient when these methods are applied to determine load distribution on a simple rectangular, straight wing planform which is the planform of most general aviation airplane. One of the examples is a straight wing planform that is shown in **Figure 1**. In this case, the calculation method from the work of Anderson was chosen to be used. The lesson learned from this testing process indicates that the simpler calculation method that can yield a result similar to the other methods will be very useful.

This article discusses the rapid estimation method of lift force distribution along wingspan by using tabulation data that is generated from lifting-line theory. This method is simpler and easier to use when compared to the other methods. It can be applied for a tapered wing which has no sweep angle and has no geometric and aerodynamic twist along wingspan. The flow condition of the wing is incompressible flow or at Mach number lower than 0.3. The range of wing aspect ratio is 4 to 12 and tapered ratio is 0.1 to 1.0.

Because lifting line theory is based on inviscid incompressible flow assumption, therefore the presented method can be used only in the condition that viscosity does not dominate the flow field or at low to moderate angle of attack which has no flow separation on wing surface.

However, the presented method can be extended to be used at subsonic compressible flow condition. This can be done by using Prandtl-Glauert rule which the detail is also discussed in this article.

2. Theory

2.1 Lifting line theory

Lifting line theory was created by Prandtl in the previous century. He proposed that a straight wing at incompressible flow condition can be considered by placing an infinite number of horseshoe vortex on the wingspan. The strength of horseshoe vortex (Γ) varies along the wingspan which represents a variation of circulation that generates lift force in the spanwise direction of a wing. In the case of general load distribution, the variation of Γ can be represented in the form of Fourier sine series as shown in the Eq. (1).

$$\Gamma(\theta) = 2bU_\infty \sum_{n=1}^{N} A_n \sin n\theta \qquad (1)$$

Which b is the length of wingspan. U_∞ is an air freestream velocity.

The variable θ represent position along wingspan which relates to the coordinate on a wing spanwise direction (y) as shown in **Figure 2**. The relation between these two parameters can be shown as in Eq. (2).

$$\mathrm{y} = (b/2)cos\theta \qquad (2)$$

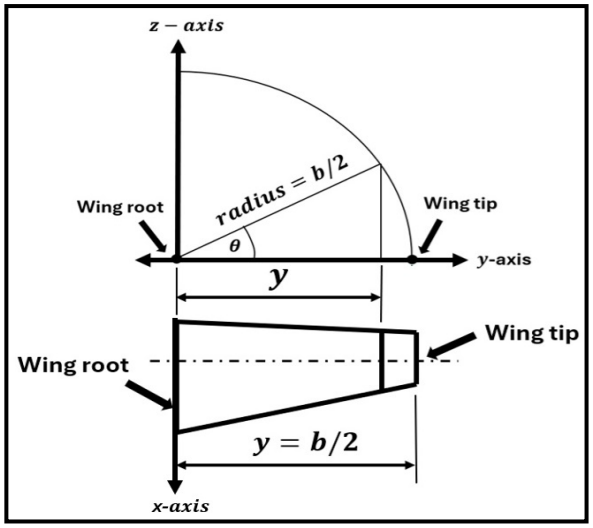

Figure 2 Shows the coordinate on the wingspan and relation between the location along wingspan (y) and θ.

The Eq. (1) can be combined with the induced angle of attack equation and theoretical lift coefficient equation for a wing cross section [7] which yields an equation that is called monoplane equation that can be shown as

$$\sum_{n=1}^{N} A_n \sin n\theta \,(\mu n + sin\theta) = \mu(\alpha - \alpha_{L=0})sin\theta \qquad (3)$$

The variable α is a geometric angle of attack of wing and $\alpha_{L=0}$ is the local zero-lift angle of attack of wing cross section. The variable μ is a product between local chord length (c), lift-slope of local wing cross section (a_0) and wingspan (b) which can be described in Eq. (4).

$$\mu = \frac{ca_0}{4b} \qquad (4)$$

The monoplane equation can be solved when the wing shape parameters are known. These parameters are wingspan, geometric angle of attack, local zero-lift angle of attack and local chord length of wing cross section. With these parameters, the Eq. (3) can be solved and the coefficient A_n can be found. Then the distribution of local lift force per unit span (l) can be determined by using Eq. (5).

$$l = \rho_\infty U_\infty \Gamma(\theta) = 2b\rho_\infty {U_\infty}^2 \sum_{n=1}^{N} A_n \sin n\theta \qquad (5)$$

Which ρ_∞ is air density.

2.2 Solving the monoplane equation

For a clean wing condition, spanwise lift distribution is always symmetrical along the wing root axis. Therefore, it can be considered by using only one side of wing and only the odd term in the series are used (n=1,3,5,7….) in the consideration. Multiple locations on the wingspan are selected and the value of θ can be found by using Eq. (2). At these selected points, all wing cross section parameters that mentioned earlier are used. Then, by using Eq. (3), the

system of linear equations can be created as shown in Eq. (6).

$$\begin{bmatrix} K_{11} & K_{12} \dots K_{1N} \\ K_{21} & K_{22} \dots K_{2N} \\ & \cdot \\ & \cdot \\ & \cdot \\ K_{N1} & K_{N2} \dots K_{NN} \end{bmatrix} \begin{Bmatrix} A_1 \\ A_2 \\ \cdot \\ \cdot \\ \cdot \\ A_N \end{Bmatrix} = \begin{Bmatrix} RHS_1 \\ RHS_2 \\ \cdot \\ \cdot \\ \cdot \\ RHS_N \end{Bmatrix} \quad (6)$$

Which K_{ij} and RHS_i are the product of the term $\sin n\theta\,(\mu n + sin\theta)$ and $\mu(\alpha - \alpha_{L=0})sin\theta$ in the Eq. (3), respectively.

This system of linear equations can be solved by using basic mathematical methods such as direct elimination method, LU factorization method or others [8]. When all of coefficients A_n are found, the local lift force along wingspan can be determined by using Eq. (5) and local cross section lift coefficient (c_l) can be calculated by

$$c_l = \frac{l}{\frac{1}{2}\rho_\infty {U_\infty}^2 c} \quad (7)$$

When the distribution of local lift coefficient is known, the wing lift coefficient can be determined by the Eq. (8) and the total lift of the wing (L) can be found by using Eq. (9)

$$C_L = \frac{b}{s}\int_{\eta=0}^{\eta=1.0} c c_l \, d\eta \quad (8)$$

$$L = \frac{1}{2}\rho_\infty {U_\infty}^2 S C_L \quad (9)$$

The parameter η is dimensionless lateral coordinate which can be described as

$$\eta = \frac{y}{b/2} \quad (10)$$

2.3 Local chord length of the rectangular wing planform

The general semi-rectangular wing planform that has no sweep angle at a quarter-chord line can be shown in **Figure 3**.

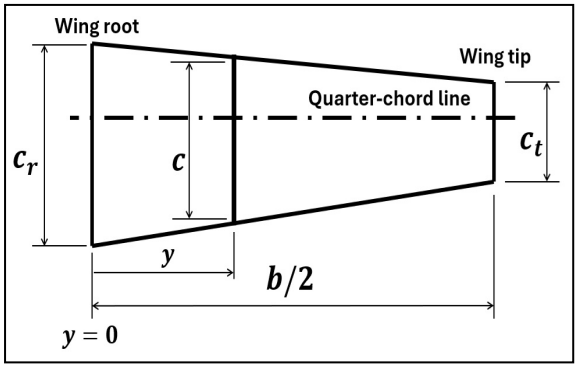

Figure 3 The shape of the rectangular wing planform that has no sweep angle at the quarter-chord line.

In many cases, the chord length at the wing tip is smaller than at the wing root. This causes a variation of the local chord length (c) along the wingspan which can be found by using Eq. (11).

$$\frac{c}{c_r} = 1 - \eta(1 - \lambda) \quad (11)$$

Which c_r and c_t are the chord length at the wing root and wing tip, respectively. The variable λ is taper ratio which can be expressed as

$$\lambda = c_t / c_r \quad (12)$$

3. Tabular data from lifting-line

3.1 Concept

The distribution of lift per unit span can be considered by using non-dimensional parameter c_l/C_L which is the ratio between local lift coefficient and wing lift coefficient. This approach is choosen because the value of c_l/C_L mainly depends on aspect ratio (AR), which can be expressed as in the Eq. (13), and taper ratio (λ).

$$AR = \frac{b^2}{S} \quad (13)$$

Which S is wing area.

Although the distirbution of local lift coefficient (c_l) along a wingspan and the value of wing lift coefficient (C_L) depend on the wing geometric angle of attack (α) and zero-lift angle of attack ($\alpha_{L=0}$), the variable c_l/C_L does not depend on these two variables. This can be explained in detail as follow.

From Anderson, the local lift coefficient distribution is determined by combining two components, the basic lift coefficient ($c_{l,b}$) and additional lift coefficient ($c_{l,a}$). For the case in this article, which considers a straight-wing that has no both geometric twist and aerodynamic twist along the wingspan, the basic lift coefficient can be discarded and local lift distribution can be determined by using additional lift coefficient only. This can be expressed as

$$c_l = c_{l,a} = C_L c_{l,a1} \quad (14)$$

Which $c_{l,a1}$ is additional lift coefficient at condition $C_L = 1.0$.

Then Eq. (14) can be rearranged as shown in Eq. (15).

$$c_l/C_L = c_{l,a1} \quad (15)$$

The variable $c_{l,a1}$ can be determined by using only wing geometric parameters which are local chord length (c), wing area (S), wingspan (b), taper ratio (λ) and aspect ratio (AR). All of these parameters are used to find coefficient in the tables and in mathematical formula to calculate $c_{l,a1}$. By carefully considering

this calculation process, it indicates that the distribution of c_l/C_L depends mainly on wing geometric parameters and does not depend on both angle of attack and zero-lift angle of attack.

The same conclusion can also be found by considering the calculation process in the work of DeYoung. In this case, the distribution of c_l/C_L can be determined by using Eq. (16).

$$c_l/C_L = K_n\left\{\frac{1+\lambda}{1(1-\eta(1-\lambda))}\right\} \quad (16)$$

Which K_n is spanwise loading coefficient.

The value of K_n can be found by using taper ratio, ascpect ratio and sweep angle at quarter-chord ($\Lambda_{c/4}$) which is set to be zero for a straight-wing planform. By using these parametes as the input, K_n at the selected positions along wingspan can be found by using the graphs that provided in this paper. Then, c_l/C_L can be determined. By considering this process, it also leads to the same conclusion that the distribution of c_l/C_L along wingspan depends mainly on wing geometric parameters only and does not depend on both angle of attack and zero-lift angle of attack.

This conclusion can also be confirmed by using lifting-line theory. In this case, for demonstration purpose, the two different straight-wings planform are created. The first one is a wing that has symmetrical airfoil profile, NACA0012. Another one has camber airfoil profile, NACA23015. For simplicity, these two wings will be refered as symmetrical wing and camber wing, respectively. The information of these two wings shows in **Table 1**.

Table 1 The basic data of two straight-wing planform

Symmetrical wing	Camber wing
NACA0012	NACA23015
$\alpha_{L=0} = 0.0^o$	$\alpha_{L=0} = -1.09^o$
$c_r = 1.24$	$c_r = 3.85$
$c_t = 0.62$	$c_t = 1.925$
$b = 7.0122$ m	$b = 21.772$ m
$S = 6.5213$ m^2	$S = 62.8659$ m^2

From the condition that there is no geometrical twist along wingspan, therefore the local geometric angle of attack at each location is the same. For the condition that there is no aerodynamic twist, this indicates that the zero-lift angle of attack along the wingspan is also the same which also implies that the cross-section profile is the same from root to tip.

Although the dimensions of these two wings are difference, the taper ratio and aspect ratio are the same which are 0.5 and 7.54, respectively. The information in **Table 1** is used as an input data for a lifting-line calculation to determine the distribution of local lift coefficient and wing lift coefficient at various angle of attack. The values of wing lift coefficient at each angle of attack from lifting-line shows in **Table 2** and the distribution of local lift coefficient for each case shows in **Figure 4**. In this calculation, the values of angle of attack are chosen to represent the range of low to moderate wing lift coefficient.

Figure 4 shows that the distribution of local lift coefficient at each angle of attack of these two wings are difference and wing lift coefficient are also not the same in all cases. However, by using this data, c_l/C_L of each case can be calculated and the result shows in **Figure 5**. This figure clearly shows that the distribution of c_l/C_L along the wingspan of both wings coincide with each other very well.

Table 2 The result from lifting-line for both wings.

α (degree)	C_L	
	Symmetrical	Camber
1.0	0.0857	0.1791
3.5	0.2999	0.3933
7.4	0.6341	0.7318

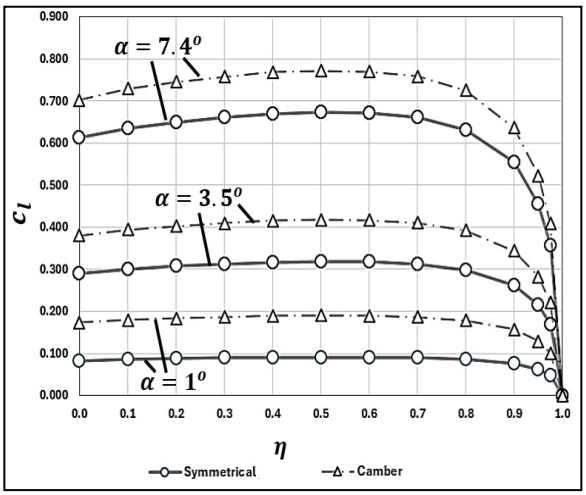

Figure 4 Shows the calculation result from lifting-line theory for symmetrical and camber wing.

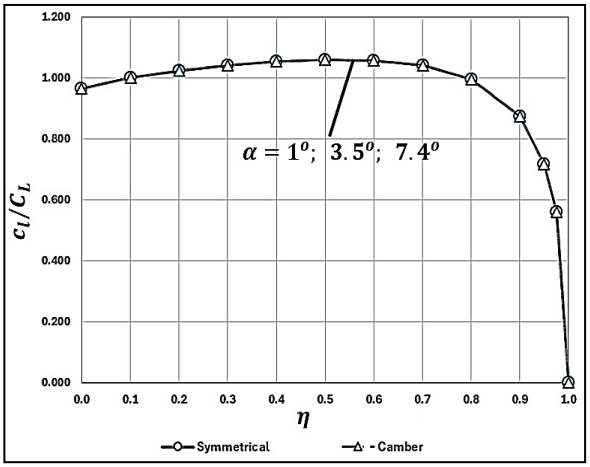

Figure 5 The distribution of c_l/C_L for both two wings.

By carefully considering all of these, it clearly shows that the distribution of c_l/C_L along wingspan of a straight-wing that has no both geometrical twist and aerodynamic twist does not depend on both angle of attack and zero-lift angle of attack but mainly depends on wing geometric

parameters which are taper ratio and aspect ratio. This indicates that it is possible to use lifting-line method to calculate c_l/C_L for a straight-wing at each taper and aspect ratio and arranges this data into a tabular form. Then, it can be used to determine c_l/C_L and span load distribution of other wing that has the same geometric condition. These tables are general and can be applied to any zero-lift angle of attack.

By using this calculation approach to determine load distribution on the wingspan, the complexity of the calculation process is largely reduced when compare to other methods. The process is easy to apply and also be able to perform manually without using a computer.

3.2 Construction of the tables

The value of c_l/C_L distribution for each aspect ratio and taper ratio for a rectangular wing planform is presented in **Table 3**–**10**. These are generated by solving the Eq. (3) to determine coefficient A_n and the value of c_l/C_L is calculated by the method discussed in the previous sections. Because the solution from the Eq. (3) is heavily influenced by the number of terms in the series and the suggested number is about 6 to 8 terms [9]. Therefore, the number of terms that are used in the Eq. (3) is 9.

Although angle of attack and zero-lift angle of attack do not have any effect on the value of c_l/C_L, these two value are still needed to complete the calculation process. Therefore, the zero-lift angle of attack is set at 0° and angle of attack is set at 5°.

The range of wing aspect ratio in the tables varies from 4 to 12 and taper ratio is at 0.1 to 1.0, which is considered to be enough to be used for a general aviation wing planform.

Each table represents the value of c_l/C_L at each position (η) along the semi-wingspan. The increment of η from **Table 3**–**7** is 0.2. However, because the value of c_l/C_L always change rapidly at the wing tip area, the increment of η around the wing tip area are reduced to 0.1, 0.5 and 0.25, respectively. Because there is no lift force generated at the wing tip, therefore the value of c_l/C_L at wing tip is always zero.

Table 3 Value of c_l/C_L at position $\eta = 0.0$

AR / λ	4	6	8	10	12
0.1	0.7876	0.8116	0.8298	0.8442	0.8561
0.2	0.8286	0.8475	0.8620	0.8737	0.8833
0.3	0.8720	0.8857	0.8964	0.9050	0.9122
0.4	0.9161	0.9244	0.9311	0.9366	0.9413
0.5	0.9601	0.9629	0.9655	0.9679	0.9699
0.6	1.0036	1.0009	0.9993	0.9984	0.9979
0.7	1.0464	1.0380	1.0323	1.0281	1.0249
0.8	1.0884	1.0743	1.0643	1.0569	1.0511
0.9	1.1297	1.1097	1.0954	1.0846	1.0763
1.0	1.1701	1.1441	1.1255	1.1115	1.1005

Table 4 Value of c_l/C_L at position $\eta = 0.2$

AR / λ	4	6	8	10	12
0.1	0.9087	0.9256	0.9374	0.9461	0.9527
0.2	0.9375	0.9490	0.9572	0.9632	0.9678
0.3	0.9682	0.9746	0.9791	0.9824	0.9849
0.4	0.9988	1.0004	1.0014	1.0020	1.0024
0.5	1.0286	1.0255	1.0232	1.0213	1.0197
0.6	1.0571	1.0497	1.0442	1.0399	1.0364
0.7	1.0845	1.0729	1.0643	1.0577	1.0525
0.8	1.1105	1.0949	1.0835	1.0747	1.0677
0.9	1.1353	1.1158	1.1016	1.0908	1.0822
1.0	1.1588	1.1357	1.1189	1.1061	1.0960

Table 5 Value of c_l/C_L at position $\eta = 0.4$

AR / λ	4	6	8	10	12
0.1	1.0230	1.0249	1.0253	1.0251	1.0246
0.2	1.0320	1.0308	1.0293	1.0278	1.0265
0.3	1.0437	1.0398	1.0366	1.0339	1.0316
0.4	1.0560	1.0499	1.0452	1.0414	1.0382
0.5	1.0682	1.0603	1.0542	1.0493	1.0453
0.6	1.0799	1.0704	1.0631	1.0574	1.0527
0.7	1.0911	1.0803	1.0719	1.0653	1.0599
0.8	1.1017	1.0896	1.0804	1.0730	1.0669
0.9	1.1117	1.0986	1.0884	1.0803	1.0737
1.0	1.1211	1.1071	1.0961	1.0874	1.0802

Table 6 Value of c_l/C_L at position $\eta = 0.6$

AR / λ	4	6	8	10	12
0.1	1.1404	1.1188	1.1027	1.0902	1.0802
0.2	1.1138	1.0965	1.0835	1.0733	1.0652
0.3	1.0949	1.0812	1.0707	1.0625	1.0559
0.4	1.0807	1.0702	1.0620	1.0554	1.0500
0.5	1.0698	1.0621	1.0558	1.0507	1.0463
0.6	1.0613	1.0561	1.0515	1.0476	1.0441
0.7	1.0546	1.0516	1.0486	1.0457	1.0430
0.8	1.0493	1.0483	1.0466	1.0446	1.0426
0.9	1.0451	1.0459	1.0454	1.0442	1.0427
1.0	1.0417	1.0442	1.0447	1.0442	1.0433

Table 7 Value of c_l/C_L at position $\eta = 0.8$

AR / λ	4	6	8	10	12
0.1	1.2707	1.2193	1.1838	1.1578	1.1379
0.2	1.1622	1.1347	1.1150	1.1002	1.0886
0.3	1.0851	1.0733	1.0645	1.0575	1.0519
0.4	1.0284	1.0275	1.0264	1.0252	1.0240
0.5	0.9851	0.9922	0.9969	1.0001	1.0024
0.6	0.9513	0.9645	0.9737	0.9803	0.9852
0.7	0.9244	0.9424	0.9551	0.9644	0.9715
0.8	0.9024	0.9243	0.9399	0.9515	0.9603
0.9	0.8843	0.9094	0.9274	0.9408	0.9511
1.0	0.8693	0.8970	0.9170	0.9320	0.9435

Table 8 Value of c_l/C_L at position $\eta = 0.9$

AR / λ	4	6	8	10	12
0.1	1.3106	1.2495	1.2085	1.1791	1.1571
0.2	1.1063	1.0884	1.0761	1.0672	1.0604
0.3	0.9802	0.9840	0.9873	0.9901	0.9923
0.4	0.8956	0.9118	0.9245	0.9345	0.9426
0.5	0.8351	0.8593	0.8781	0.8930	0.9051
0.6	0.7900	0.8196	0.8426	0.8610	0.8760
0.7	0.7551	0.7887	0.8148	0.8357	0.8528
0.8	0.7275	0.7640	0.7925	0.8153	0.8341
0.9	0.7052	0.7440	0.7743	0.7986	0.8187
1.0	0.6868	0.7274	0.7592	0.7848	0.8058

Table 9 Value of c_l/C_L at position $\eta = 0.95$

AR / λ	4	6	8	10	12
0.1	1.2451	1.1945	1.1616	1.1385	1.1213
0.2	0.9654	0.9647	0.9661	0.9684	0.9708
0.3	0.8173	0.8358	0.8515	0.8650	0.8765
0.4	0.7257	0.7536	0.7767	0.7961	0.8126
0.5	0.6637	0.6969	0.7242	0.7471	0.7666
0.6	0.6190	0.6555	0.6854	0.7106	0.7322
0.7	0.5854	0.6240	0.6558	0.6825	0.7055
0.8	0.5593	0.5995	0.6325	0.6603	0.6842
0.9	0.5385	0.5798	0.6138	0.6424	0.6671
1.0	0.5216	0.5637	0.5984	0.6277	0.6529

Table 10 Value of c_l/C_L at position $\eta = 0.975$

AR / λ	4	6	8	10	12
0.1	1.0881	1.0591	1.0424	1.0322	1.0256
0.2	0.7842	0.7971	0.8100	0.8221	0.8334
0.3	0.6418	0.6675	0.6900	0.7098	0.7275
0.4	0.5588	0.5898	0.6165	0.6398	0.6603
0.5	0.5045	0.5382	0.5669	0.5920	0.6141
0.6	0.4663	0.5014	0.5313	0.5573	0.5803
0.7	0.4381	0.4740	0.5045	0.5312	0.5547
0.8	0.4164	0.4528	0.4838	0.5108	0.5346
0.9	0.3993	0.4360	0.4673	0.4945	0.5186
1.0	0.3854	0.4224	0.4538	0.4812	0.5054

4. Illustrative example

4.1 Lift force per unit span distribution

To demonstrate how to use the data from the tables to estimate lift distribution on wing, an example that shows the calculation process is discussed in this section. A straight-rectangular wing planform has the geometric parameters as follow

Wingspan (b)	10.18	m
Wing area (S)	15.5	m^2
Wing chord length at root (c_r)	2.03	m
Wing chord length at tip (c_t)	1.015	m
Wing zero-lift angle of attack	-2.1°	
Wing angle of attack	3.9°	
Air velocity	198	km/h
Air density at altitude	0.81912	kg/m^3

From this information, the wing aspect ratio and taper ratio can be determined by using Eq. (12)–(13) which are 6.686 and 0.5, respectively. The value of wing lift coefficient C_L is determined by

$$C_L = a(\alpha - \alpha_{L=0}) \tag{17}$$

Which a is a lift-slope of a straight wing in 1/degree that can be theoretically approximated by

$$a = \frac{a_0}{1+\frac{a_0}{\pi e_1 (AR)}} \times 0.0174 \tag{18}$$

Which a_0 is the lift-slope of wing cross-section profile. In general, its value usually be assumed to be 2π. Variable e_1 is a wing geometric factor which is typically in range about 0.95. By using Eq. (17)–(18) with the wing geometric parameters, lift coefficient of this wing is 0.5.

Because the value of aspect ratio lies between 6 and 8 in the tables, therefore the interpolation process is used to find the value of c_l/C_L at all position of η. The result is shown in **Table 11** and the lift distribution is shown in **Figure 6**. In this table, it also shows the size of local chord length which is calculated by the Eq. (11) and the distribution of lift per unit span calculated from the Eq. (7).

Table 11 Value of c_l/C_L at each position on wingspan

η	c_l/C_L	c_l	c (m)	l (N/m)
0.000	0.9638	0.4819	2.0300	1,211.98
0.200	1.0247	0.5124	1.8270	1,159.71
0.400	1.0582	0.5291	1.6240	1,064.55
0.600	1.0599	0.5299	1.4210	932.98
0.800	0.9938	0.4969	1.2180	749.82
0.900	0.8657	0.4329	1.1165	598.74
0.950	0.7063	0.3532	1.0658	466.29
0.975	0.5445	0.2722	1.0404	350.91
1.000	0.0000	0.0000	1.0150	0.00

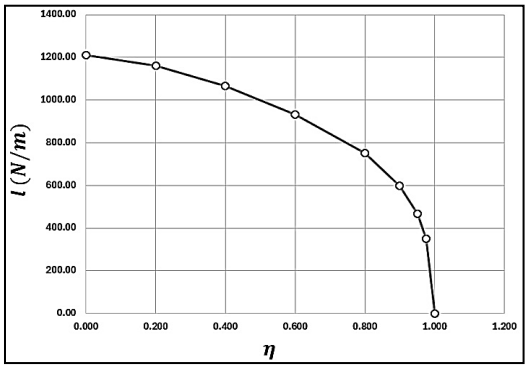

Figure 6 Shows the calculation result from the example.

4.2 Total lift force on a semi-wingspan

From the lift distribution graph as shown in **Figure 7**, the relation between the total lift force of a semi-wingspan (L') and lift per unit span can be written in differential form as

$$dL' = l\,dy \tag{19}$$

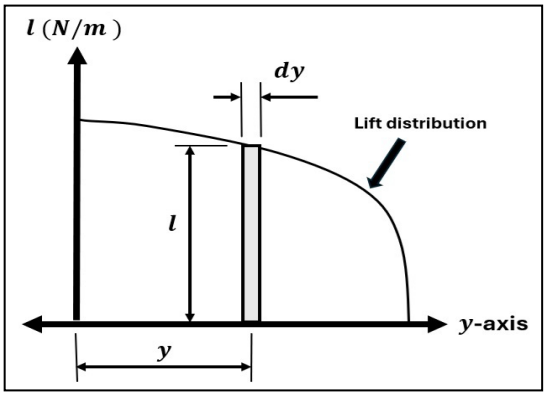

Figure 7 The distribution of lift per unit span along the semi wingspan.

From the Eq. (10), the coordinate y can be transformed to η by using

$$dy = (b/2)\,d\eta \tag{20}$$

When substitutes Eq. (20) into Eq. (19) and perform integration process, the result can be shown as

$$L' = \frac{b}{2}\int_{\eta=0}^{\eta=1.0} l\,d\eta \tag{21}$$

Because the data of lift distribution comes into a tubular form as shown in **Table 11**. Therefore, numerical integration is needed for the calculation. In this case, the trapezoid rule is chosen. Then, the Eq. (21) becomes

$$L' = \frac{b}{2}\sum_{i=1}^{N-1}\frac{(l_{i+1}+l_i)}{2}\Delta\eta \tag{22}$$

When applied the Eq. (22) to the data from **Table 11**, the result shows that the total lift force of a semi-wingspan in this example is 4.765 kN. However, this value is calculated by considering only on a semi-wingspan. Therefore, the magnitude of total lift force for the entire wing can be found by multiplying the result from Eq. (22) by two which, in this case, is 9.531 kN.

4.3 Calculation of spanwise center of pressure

The spanwise center of pressure ($\bar{\eta}$) is the location of the total lift force measured from wing root. This position can also be determined by using the data in **Table 11**. It can be done by considering the moment along x-axis, as shown in **Figure 2**, at wing root. The relation between lift per unit span and moment can be shown in Eq. (23).

$$dM_{root} = ly\,dy \tag{23}$$

Then, the location of the total lift force of a semi-wingspan in y coordinate can be found by

$$\bar{y} = \frac{1}{L'}\int_{y=0}^{y=b/2} ly\,dy \tag{24}$$

Using the relation in Eq. (10) and Eq. (20), the Eq. (24) can be transformed in to η as

$$\begin{aligned}(b/2)\bar{\eta} &= \frac{1}{L'}\int_{y=0}^{y=b/2} l\left(\frac{b}{2}\eta\right)\,d\left(\frac{b}{2}\eta\right)\\ \bar{\eta} &= \frac{b}{2L'}\int_{\eta=0}^{\eta=1.0} l\eta\,d\eta\end{aligned} \tag{25}$$

As in the previous section, the trapezoid rule is chosen for the calculation process. Then the Eq. (25) becomes

$$\bar{\eta} = \frac{b}{2L'}\sum_{i=1}^{N-1}\left[\frac{(l_{i+1}+l_i)\Delta\eta}{2}\right]\left[\frac{\eta_{i+1}+\eta_i}{2}\right] \tag{26}$$

When applied Eq. (26) to calculate data in the **Table 11**, the result shows that the value of $\bar{\eta}$ is at 0.4317 of a semi-wingspan length or at 2.198 m measured from the wing root position.

5. Comparison

5.1 Comparison of lift distribution with the result from other calculation methods

The calculation method for lift distribution from Anderson and DeYoung are also used to determine lift distribution of the wing in this example. The results from these two methods are compared to the result in **Table 11** and is shown in **Figure 8**.

When compared the result from present method with the result from the Anderson's method, the maximum difference of local lift per unit span at location $\eta = 0$ to 0.9 is 5.721 percent. At the location from $\eta = 0.9$ to 1.0, the maximum difference is 9.801 percent.

In the case of DeYoung, the maximum difference is 5.587 percent at the location $\eta = 0$ to 0.9. However, this value rises to 25.701 percent at the wing tip area. This drastically rise occurs because the DeYoung's method considers location $\eta = 0.9239$ as a last position for the calculation process but the present method considers the location further from this point which are at $\eta = 0.95$ and 0.975. Therefore, this leads to a large difference between these two results around wing tip area which can be noticeable in **Figure 8**.

5.2 Spanwise center of pressure and total lift force

The location of spanwise center of the wing in present method can also be determined by using the data in the work of DeYoung. The result shows that the location of spanwise center of pressure is 0.424 of a semi-wingspan length, measured from the wing root. This value differs from the result that discussed in section 4.3 only 1.8 percent.

The total lift force of a semi-span wing also be determined by using the method suggested in Nui [10] which the result is 4.771 kN. When compared with the result from the present method in section 4.2, which is 4.765 kN, the difference between these two results is only 0.125 percent.

These two results show that the present method can also give a result for spanwise center of pressure and total lift force that agrees very well with other calculation methods.

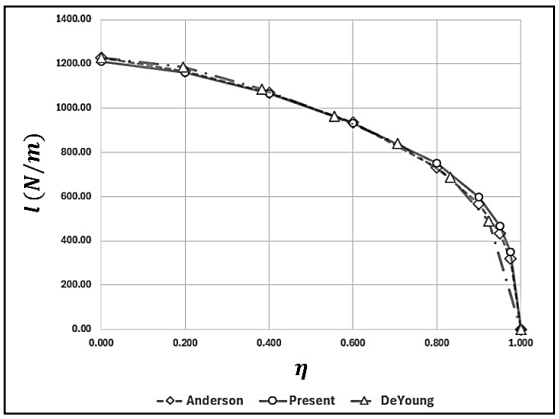

Figure 8 Comparison the results from three calculation methods.

5.3 Comparison with experimental data

The data from the experimental study is used to compare with the result from the present calculation method. The data comes from the work of Jacobs [11] which studied pressure distribution of various types of wing planform in the wind tunnel. In this case, the data of a rectangular wing planform that has zero sweep angle is chosen for the comparison. This wing has a constant chord length 0.15 m and has its wingspan 0.77 m. The taper ratio and aspect ratio are 1.0 and 5.133, respectively. The dynamic pressure at the testing condition is 950 Pa. The angle of attacks are 5.6 and 11.4 degrees and wing lift coefficient are 0.483 and 0.683, respectively. By using **Table 3–10** and wing lift coefficients from the experimental data, the lift distribution is determined. The comparison of lift distribution along semi-wingspan of these two cases and the calculation results are shown in **Figure 9** and **Figure 10**. These graphs clearly show that the result from the presented calculation method also agrees very well with the experimental data.

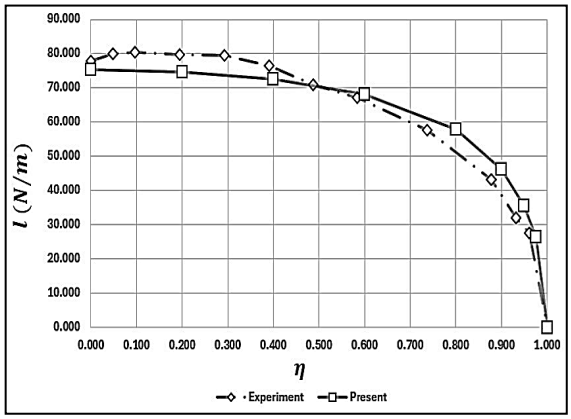

Figure 9 Comparison the calculation results with the experimental data at angle of attack 5.6 degree.

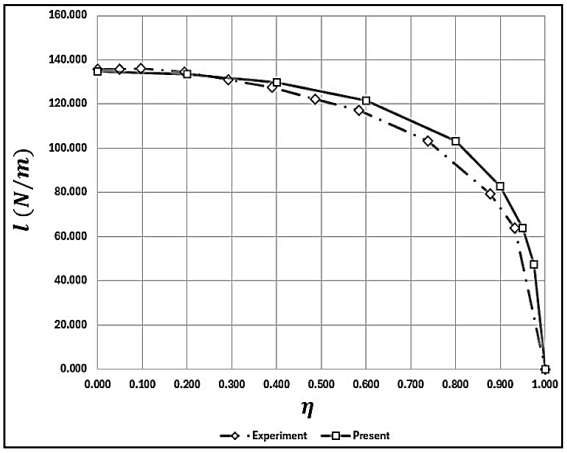

Figure 10 Comparison the calculation results with the experimental data at angle of attack 11.4 degree.

6. Compressibility effect

Although the present method is based on inviscid incompressible flow theory, it can be extended to be used for compressible flow condition. This can be done by using the Prandtl-Glauert rule.

The Prandtl-Glauert states that the two-dimensional lift coefficient (c_l) of a slender body at each Mach number for subsonic flow condition can be determined by using the relation

$$c_l = \frac{c_{l,0}}{\sqrt{1 - {M_\infty}^2}} \tag{27}$$

Which $c_{l,0}$ is a two-dimensional lift coefficient at incompressible flow condition and M_∞ is free-stream Mach number.

To determine spanwise lift distribution at each Mach number, first lift coefficient distribution along wingspan is calculated by using method discussed in the previous sections. By using these values of lift coefficient as $c_{l,0}$, lift coefficient at each Mach number can be determined by applying the Eq. (27).

For demonstration, the presented calculation method is applied to determine lift distribution on a high aspect ratio wing at Mach number 0.4 and 0.6. This wing has an aspect ratio 9.18, the taper ratio is 0.4 and the angle of attack is 4°. The data of semi-span lift distribution of this wing comes from the study of Whitcomb [12]. The comparison between the results from the calculation method and the data from the experiment is shown in **Figure 11**. This figure clearly shows that the result from the presented method agrees very well with the experimental data at both Mach number 0.4 and 0.6 condition.

However, it should be noted that there is a limitation to this presented method. Because the Prandtl-Glauert rule can be used very well at free-stream Mach number lower than critical Mach number, therefore the presented method must also be applied in this range too.

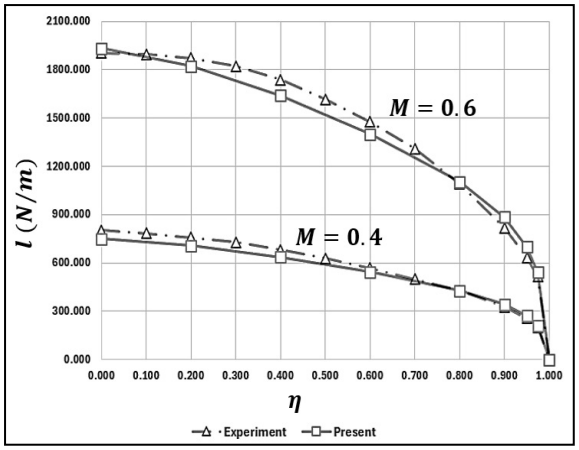

Figure 11 Comparison local lift distribution from the present calculation method with the experimental data of a high aspect ratio wing at Mach number 0.4 and 0.6.

7. Conclusion

The rapid estimation method of the spanwise lift distribution of a rectangular wing planform is discussed in this article. This method is based on the use of the tabular data that is generated by lifting line theory. This calculation method is easier to use but can yield a result similar to the other more complex methods. Although the presented method is based on the assumption of incompressible flow condition or at Mach number lower than 0.3, it can be extended to be used for compressible flow condition by using the Prandtl-Glauert rule.

For lift distribution, the present method can give the result that differs from other methods in range about 5 to 6 percent in the most location along wingspan. However, this value can be higher at wing tip area.

In case of total lift force and spanwise center of pressure, the result from present method differs from other method only 1.8 and 0.125 percent, respectively.

However, the present method still has some limitations. It can be used only for a rectangular wing that has zero sweep angle, has no geometric and aerodynamic twist along wingspan only and the wing tip must be a straight shape. For a compressible condition, this method can be applied only at free-stream Mach number lower than critical Mach number which comes from the limitation of Prandtl-Glauert rule.

8. References

[1] S. Chinvorarat, B. Watjatrakul, P. Nimdum, T. Sangpet, T. Soontornpasatch and P. Vallikul, "Static testing for composite wing of a two-seat airplane," *in 9th TSME-International Conference on Mechanical Engineering (TSME-ICoME 2018)*, Phuket, Thailand, Dec. 11–14, 2018, pp. 1–8, doi:10.1088/1757-899X/501/1/012026

[2] R. F. Anderson, "Determination of the characteristics of tapered wings," National Advisory Committee for Aeronautics, Washington, WA, USA, Rep. NACA-TR-572, 1937.

[3] J. Deyoung, "Theoretical Additional Span Loading Characteristics of Wings with Arbitrary Sweep, Aspect Ratio, and Taper Ratio," National Advisory Committee for Aeronautics, Washington, WA, USA, Rep. NACA-TN-1491, 1947.

[4] V. I. Stevens, "Theoretical Basic Span Loading Characteristics of Wings with Arbitrary Sweep, Aspect Ratio, and Taper Ratio," National Advisory Committee for Aeronautics, Washington, WA, USA, Rep. NACA-TN-1772, 1948.

[5] J. Weisinnger, "The lift distribution of swept-back wings," National Advisory Committee for Aeronautics, Washington, WA, USA, Rep. NACA-TM-1120, 1947.

[6] J. DeYoung and C. W. Harper, "Theoretical symmetric span loading at subsonic speeds for wings having arbitrary plan form," National Advisory Committee for Aeronautics, Washington, WA, USA, Rep. NACA-TR-921, 1948.

[7] T. Soontornpasatch, "Incompressible flow over finite wings," in *Aerodynamics for Aeronautical Engineers*, Bangkok, Thailand: KMUTNB Textbook publishing center, 2024, ch. 6, sec. 6.4, pp. 92–99.

[8] J. D. Hoffman, "System of Linear Algebraic Equations," in *Numerical Method for Engineers and Scientists*, 2nd ed, New York, NY, USA: McGraw-Hill, Inc., 2001, ch. 1, sec. 1.7, pp.59–67.

[9] J. J. Bertin and R. M. Cummings, "Incompressible Flow About Wings Of Finite Span," in *Aerodynamics for Engineers,* 5th ed., New York, NY, USA: Pearson Education Inc., 2009, ch. 7, sec. 7.3, pp. 346–347.

[10] M. C. Niu, "Aircraft loads," in *Airframe structural design: Practical design information and data on aircraft structures*, North Point, Hong Kong: Conmilit Press Ltd., 1989, ch. 3, sec. 3.11, pp. 79–80.

[11] W. Jacobs, "Pressure-distribution measurements on unyawed swept-back wings," National Advisory Committee for Aeronautics, Washington, WA, USA, Rep. NACA-TM-1164, 1947.

[12] R. T. Whitcomb, "Investigation of the characteristics of a high-aspect-ratio wing in the Langley 8-foot high-speed tunnel," National Advisory Committee for Aeronautics, Washington, WA, USA, Rep. NACA-RM-L6H28a, 1946.